Water Science & Technology

IWA PUBLISHING

Water Science & Technology Vol 89 No 7, 1879 doi: 10.2166/wst.2024.079

Treatment of tomato paste wastewater by electrochemical and membrane processes: process optimization and cost calculation

Aliye Şen[a], Ceyhun Akarsu[b], Zeynep Bilici[a], Hudaverdi Arslan[a] and Nadir Dizge[a,*]

[a] Department of Environmental Engineering, Engineering Faculty, Mersin University, Mersin, Turkey
[b] Department of Environmental Engineering, Engineering Faculty, Istanbul University-Cerrahpasa, Istanbul, Turkey
*Corresponding author. E-mail: ndizge@mersin.edu.tr

ABSTRACT

This study investigated the treatment of wastewater from tomato paste (TP) production using electrocoagulation (EC) and electrooxidation (EO). The effectiveness of water recovery from the pretreated water was then investigated using the membrane process. For this purpose, the effects of independent control variables, including electrode type (aluminum, iron, graphite, and stainless steel), current density (25–75 A/m^2), and electrolysis time (15–120 min) on chemical oxygen demand (COD) and color removal were investigated. The results showed that 81.0% of COD and 100% of the color removal were achieved by EC at a current density of 75 A/m^2, a pH of 6.84 and a reaction time of 120 min aluminum electrodes. In comparison, EO with graphite electrodes achieved 55.6% of COD and 100% of the color removal under similar conditions. The operating cost was calculated to be in the range of $0.56–30.62/m^3. Overall, the results indicate that EO with graphite electrodes is a promising pretreatment process for the removal of various organics. In the membrane process, NP030, NP010, and NF90 membranes were used at a volume of 250 mL and 5 bar. A significant COD removal rate of 94% was achieved with the membrane. The combination of EC and the membrane process demonstrated the feasibility of water recovery from TP wastewater.

Key words: cost-effectiveness analysis, electrocoagulation, electrooxidation, membrane process, optimization, tomato paste wastewater

HIGHLIGHTS

- The treatment of tomato paste wastewater via electrocoagulation (EC) and electrooxidation (EO) processes was examined.
- The membrane process was used as the post-treatment.
- Aluminum and graphite electrodes were chosen for EC and EO, respectively.

GRAPHICAL ABSTRACT

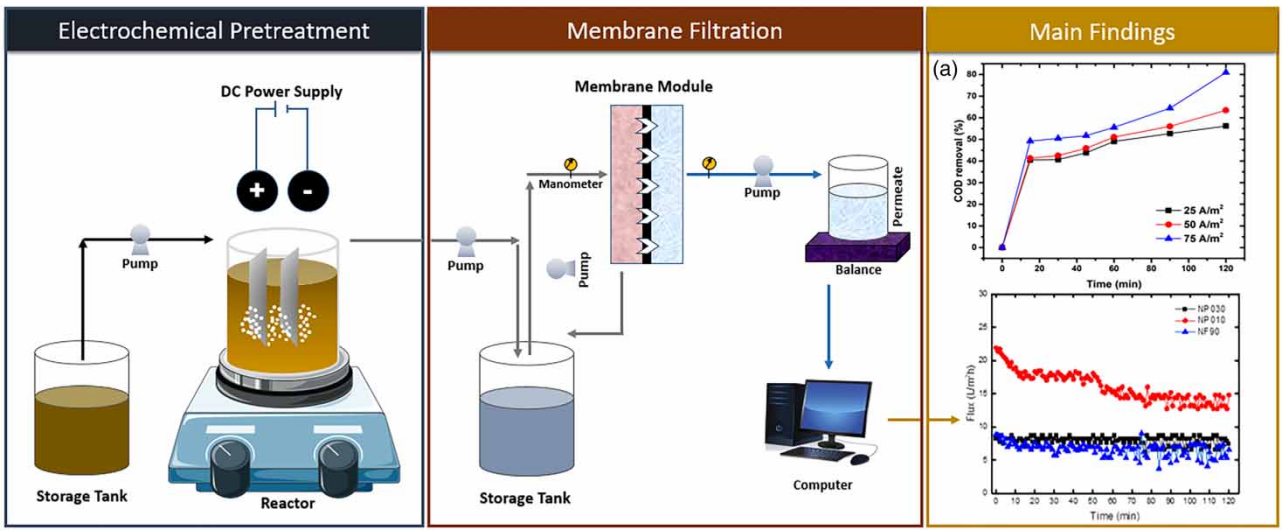

1. INTRODUCTION

Turkey is one of the five tomato paste (TP)-producing countries in the world. With the expansion of livestock in the extensive production of TP, the treatment of TP wastewater (TPW) has become an important issue. TPW is characterized by high chemical oxygen demand (COD) of 2,800–15,500 mg/L, biochemical oxygen demand (BOD) of 1,750–7,950 mg/L, total Kjeldahl nitrogen of 48–340 mg/L, and ammonium-nitrogen (NH_4^+-N) of 21–235 mg/L (Gohil & Nakhla 2006). According to Mannapperuma *et al.* (1993), about 3.5 m^3 of wastewater is generated per tonne of TP produced. However, studies on the chemical and microbiological properties and treatment options of TP are very limited. So far, only a few methods have been investigated including UV oxidation (Mahoney *et al.* 2018), combined biological treatment (Gohil & Nakhla 2006), and nanofiltration (Alghooneh *et al.* 2016) as they are highly efficient, cost-effective, and environmentally friendly. Therefore, there is a need to develop an alternative treatment process that offers high efficiency with less duration and chemical consumption as well as being easy to install.

Electrocoagulation (EC), which combines the advantages of coagulation, flotation, and electrochemistry, has been extensively studied in recent years due to its ecological versatility and has been adapted for the treatment of food processing wastewater (Sardari *et al.* 2018; Akarsu *et al.* 2021, Arslan *et al.* 2023). During the EC process, metal hydroxides, whose density is higher than that of water, settle, while floc floats by bubbles due to the neutralization of the surface charge of the pollutants (Qasem *et al.* 2021). The superior electrode is one of the control parameters that not only affects the generation of *in situ* coagulants but is also associated with the cost (Delil & Gonen 2019). In general, aluminum (Al), iron (Fe), magnesium, steel, and zinc have been used as electrode materials (Safwat 2020; Ebba *et al.* 2021; Figueiredo *et al.* 2022). Among them, Al and Fe are the most widely used due to their various properties such as low cost, non-toxicity, and high valence, which lead to the efficient removal of pollutants (Hakizimana *et al.* 2017). In electrooxidation (EO), in contrast to EC, the main function of the anode is the oxidative degradation of organic substances by the hydroxyl radicals generated at high reaction rates. Consequently, non-consumable electrodes are used in EO to attenuate pollutants directly or indirectly through the generation of oxidizing agents in solution (Lynn *et al.* 2019).

Membrane treatment systems are one of the best systems for removing pollutants and recycling water. The membrane system is widely used because it does not require chemicals for purification, is easy to operate, and has good separation properties due to its pore diameters (Majidi *et al.* 2022). The performance of the membrane system varies depending on the characterization of wastewater, pressure, and membrane type. While the pollutants that cannot pass due to the pore diameter on the membrane surface remain concentrated in the upper part, the part that passes through the membrane is taken as a filtrate (Dadari *et al.* 2022). While suspended solids and dissolved substances with a high molecular weight are retained in the membrane, water and substances with a low molecular weight pass through the membrane (Esfahani *et al.* 2019). One of the major disadvantages of the membrane system is the contamination problem. Clogging problems due to the contamination of the membrane are caused by both biological and chemical substances. If this clogging problem increases, the lifespan of the membrane is shortened (Tummons *et al.* 2020).

In recent years, EC and EO applications have been extensively studied for the treatment of industrial sewage such as textile industry (Can *et al.* 2006), olive mill (Inan *et al.* 2004), brewery (Wysocka & Masalski 2018), dairy (Reilly *et al.* 2019), acid mine (Alam *et al.* 2022), furniture industry (Vicente *et al.* 2023), and slaughterhouse (Adou *et al.* 2022). To our knowledge, however, despite these advantages of electrochemical methods, there is little literature research on the treatment of TP. The aim of this study is therefore to treat TPW using EC and EO processes. Subsequently, it is aimed to recover water by the membrane process after pretreatment under optimum conditions. In this context, control variables such as electrode combination (Al–Al, Fe–Fe, G–G, and SS–SS), current density (25, 50, and 75 A/m^2), and electrolysis time (15, 30, 45, 60, and 120 min) were analyzed to determine the optimum operating conditions for COD and color removal performance as well as on the total operating cost. For the membrane process, NP030, NP010, and NF90 membranes were used with a volume of 250 mL, a pressure of 5 bar, and an operation time of 2 h. The flux was collected every minute, and COD analysis was performed on the filtrate sample.

2. MATERIALS AND METHODS

2.1. TPW characterization and analysis

TPW used in this study was taken from a company in Mersin, Turkey. It was collected from the sewerage system in September 2022 and cooled down to 4 °C for further procedure. The specific characteristics of TPW are given in Table 1.

Table 1 | TPW characteristics

Parameter	Unit	Value
pH	-	6.84 ± 0.12
COD	mg/L	1,260 ± 82
Color	Pt–Co	150 ± 14
Conductivity	μS/cm	1,490 ± 10

The changes of COD and the color decrease depending on the electrode (Al–Al, Fe–Fe, G–G, and SS–SS), current density (25, 50, and 75 A/m^2), and electrolysis time (15, 30, 45, 60, 90, and 120 min) were observed. pH and conductivity were measured by a multi-parameter instrument (Hach-Lange HQ40d). COD of the samples was determined by the dichromatic closed reflux method of the standard methods. The color was determined at 455 nm with a spectrophotometer (Hach-DR 6000) and calibrated using the platinum–cobalt method (Pt/Co). All analyses were performed in duplicate and mean values were reported.

The removal or elimination efficiency was calculated using the following equation:

$$\text{Removal efficiency } (\%) = \frac{\text{Concentration}_{\text{initial}} - \text{Concentration}_{\text{final}}}{C_{\text{initial}}} \times 100 \quad (1)$$

2.2. Experimental setup

2.2.1. Electrochemical experiment

The laboratory setup for the electrochemical treatment tests is shown in Figure 1. The experiments were carried out in a cylindrical borosilicate reactor with a working volume of 500 mL and mixed with a magnetic stirrer (Wisd-Wisestir msh-20A, Germany) at 300 rpm. The Al–Al, Fe–Fe, G–G, and SS–SS electrodes were plate-shaped and had the dimensions of 5 cm width × 8 cm height × 1 mm thickness and an electrode spacing of 2 cm. Before each experiment, the surface of the electrodes was rinsed with acidified water and dried at 105 °C for 5 min to remove surface impurities and avoid deviations in the analytical results. A rectifier (AATech ADC-3303D, Germany) was used to transfer the required current.

2.2.2. Membrane experiment

The membrane experiment was carried out after pretreatment by the electrochemical process. The laboratory-scale electrochemical and membrane system is shown in Figure 1. A stainless steel membrane filtration system (Sterlitech HP4750 Stirred Cell) with a working volume of 300 mL and a working pressure of 69 bar was used for membrane experiments. The effective

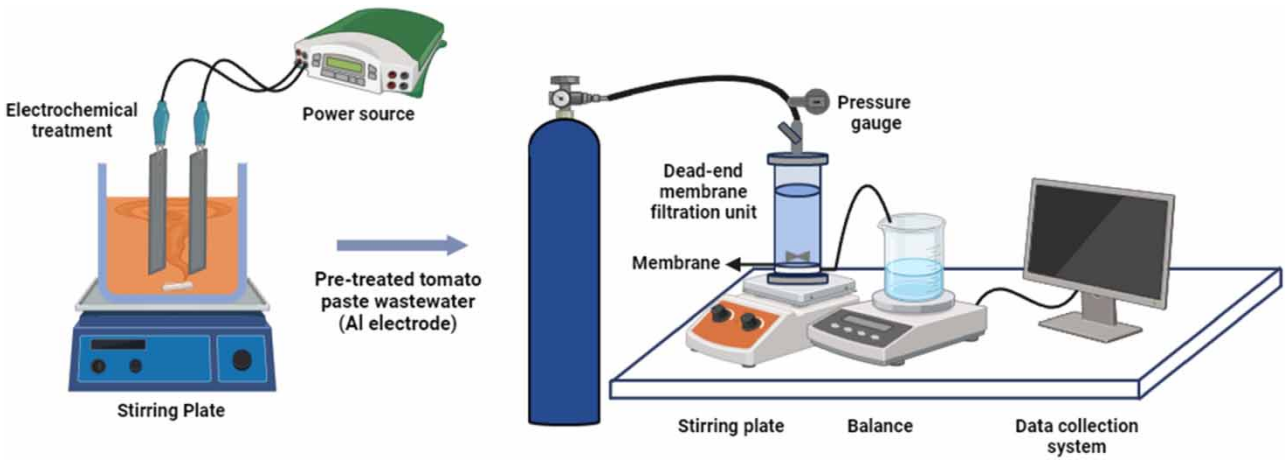

Figure 1 | Experimental setup of EC and membrane processes.

filtering area of the membrane is 14.6 cm^2. N_2 gas was used as the driving force in the membrane system. There is a magnetic stirrer in the filtration system to ensure the mixing of wastewater. In order to instantly record the permeate flux, a precision scale (FZ-3000i brand) was connected to the computer via RS-COM connection. NP030, NP010, and NP90 membranes were used in the membrane. Membranes with a diameter of 4.3 cm were cut to fit into the cell. The effective filtering area of the membrane is 14.6 cm^2. After the pretreatment of TP wastewater with electrochemical processes, water recovery performance was investigated with commercially purchased membranes. The general characteristics of membranes are given in Table 2. First, deionized water was filtered through NP030, NP010, and NP90 membranes at 5 bar operating pressure for 30 min. Then, pretreated wastewater was fed into the system. COD analyses were performed on inlet and outlet samples. The flux values obtained from the membranes were calculated using the following equation:

$$\text{Flux}(J_w) = \frac{\Delta V}{A \times \Delta t} \tag{2}$$

where J_w is the flux (L/m^2·h), ΔV is the amount of permeate sample collected over a given period of time (Δt, h) (L), and A is the membrane area used for filtration (m^2).

2.3. Cost calculation

Minimizing operating costs in wastewater treatment plants is of the utmost importance to the industry. In the context of electrochemical processes, the basic cost calculation involves the overall evaluation of electricity consumption and electrode loss. Consequently, the operating costs (OCs) associated with EC and EO processes can be determined using the following equation:

$$\text{OC} = \alpha \times C_{\text{energy}} + \beta \times C_{\text{electrode}} \tag{3}$$

where OC is the operation cost (US$/$m^3$), α represents the price of electrical energy (US$ kW/h) (0.061 US$ kW/h according to the Turkish market in January 2024), and β is the price of electrode materials ($/kg) (1.13 US$/kg Al electrode according to the Turkish market in January 2024).

Additionally, the theoretical maximum dissolved mass of the electrode, as dictated by Faraday's law, can be computed through the following equation:

$$C_{\text{electrode}} = \frac{W_{\text{initial}} - W_{\text{final}}}{\cup} \tag{4}$$

where $C_{\text{electrode}}$ is the electrode consumption (kg/m^3), W_{initial} is the weight of the electrode (kg) before the experiment, W_{final} is the weight of the electrode (kg) after the experiment, and $\cup$ is the active volume (m^3).

On the other hand, the energy consumption in the electrochemical process was calculated using the following equation:

$$C_{\text{energy}} = \frac{UIt}{\cup} \tag{5}$$

where C_{energy} is the power consumption (kWh/m^3), I is the applied current (A), U is the cell potential (V), and t is the operating time (h).

Table 2 | General properties of the membranes used in the study

Membrane	Material	Maximum temperature (°C)	pH	Pore size (Da)	Flux	Contact angle (°)	Firm
NP010	Polyethersulfone (PES)	95	0–14	~1,000	24–30 LMH/5 bar	47.3	Microdyn Nadir™
NP030	Polyethersulfone (PES)	95	0–14	~400–600	9–12 LMH/5 bar	88.5	Microdyn Nadir™
NF90	Polyamide (PA)	45	2–11	~90–180	12–15 LMH/5 bar	72	DOW Filmtec

3. RESULTS AND DISCUSSION

3.1. Electrochemical experiment

3.1.1. COD and color removal

Figure 2 shows the changes in current density and electrolysis time on the COD removal efficiency for the electrode pairs of Al–Al, Fe–Fe, G–G, and SS–SS. The COD removal efficiencies were increased in the range of 40.5–81.0, 37.5–51.1, 28.9–55.6, and 35.4–50.5% at a current of 25, 50 and 75 A/m^2 for Al–Al, Fe–Fe, G–G, and SS–SS electrodes, respectively. For all electrode pairs, the degradation of organics increased as the current density increased. This assessment is even more pronounced for aluminum. While the removal efficiency at 25 A/m^2 is 50%, the efficiency increases to 81.0% when the current density is increased to 75 A/m^2 (Figure 2(a)). However, further increasing the applied current did not result in better removal efficiency for the electrode pairs of Fe, G, and SS. It was also found that the highest removal of COD is achieved in a short time such as 15 min for Fe, G, and SS electrode pairs, and the maximum time is required with Al. Thus, it can be said that the released Al^{3+} ions leading to the formation of $Al(OH)_3$ particles are high due to the increase in current density (Deghles & Kurt 2016). Another possible reason for the high removal efficiency could be the increased bubble formation on the surface of the aluminum electrode caused by the increase in current density (Deniz & Akarsu 2018).

Operating time is another key variable in electrochemical treatment processes, as the coagulant concentration generated by electrolysis is time-bound and directly dependent on the electrical charge supplied per unit volume of EC, while the desired

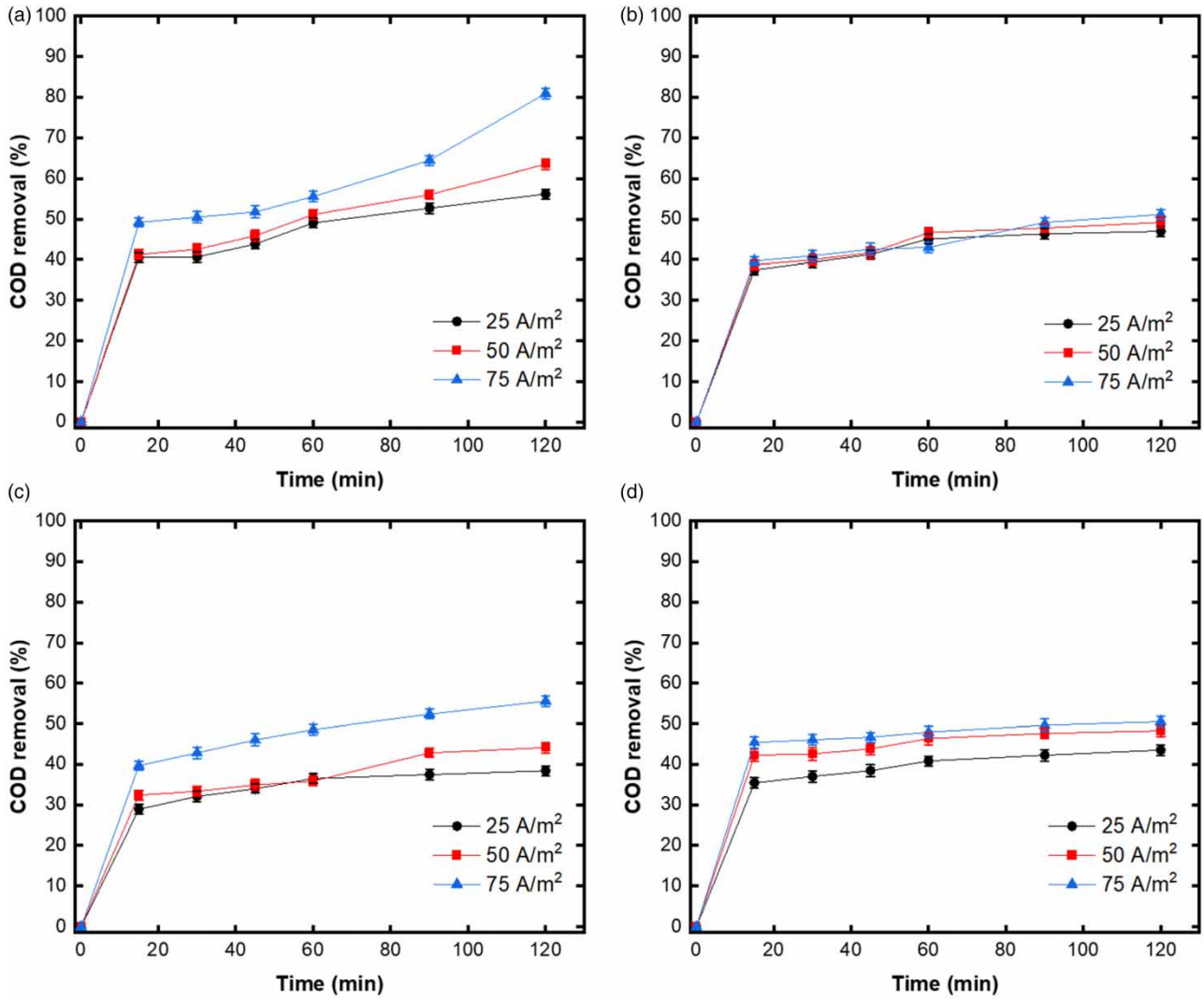

Figure 2 | Effect of operating variables on COD removal by using (a) Al–Al, (b) Fe–Fe, (c) G–G, and (d) SS–SS.

oxidation of substances with the gases O_2 and H_2 was achieved by the cathodic activity of the anode of EO (Khan *et al.* 2023). Metallic polymer types in the form of hydroxides produce more hydroxyl radicals over a longer period of time, resulting in higher removal efficiency (Asaithambi *et al.* 2016). However, the pollutant removal efficiency increases with the duration of electrolysis until it reaches saturation under optimal conditions (Can *et al.* 2014). The duration of operation is closely related to the current density and therefore needs to be optimized, as the desired removal efficiency depends on the availability of the coagulation floc for the desired pollutant removal. Therefore, the effect of electrolysis time on the process has been extensively studied in the literature. For example, Deveci *et al.* (2019) used a laboratory-scale EC to remove chromium and organics from tannery wastewater under different operating parameters and found that increasing the treatment time significantly improved removal. Similar results were found for the removal of other pollutants, e.g. total phenol (Arslan *et al.* 2023), surfactants (Akarsu *et al.* 2022), inorganics (Akbay *et al.* 2019), and COD (Delil & Gönen 2019).

After 15 min of electrochemical treatment, the color removal for the electrode pairs Al, Fe, and SS was 100%, while the maximum color removal for the G pairs was achieved in 45 min. Similarly, several studies also report that different Fe and Al electrode arrangements were effectively used in color removal (Majlesi *et al.* 2016; Dizge *et al.* 2018). As expected, in the case of Al, Fe, and SS electrode pairs, not only phase transfer but also redox reactions can contribute to color removal (Kabdasli *et al.* 2009).

3.1.2. Effect of electrolysis time on pH changes

The pH value of the environment also changes the reactions that take place in the reactor. Because of these changes, it is difficult to control the pH of the process with adequate performance. However, if you follow the measurements of the pH distribution in the reactor, you will usually get an idea of the reactions that are taking place. For example, if the initial pH of the solution is below 7, an increase in pH is expected as the process progresses (Arslan *et al.* 2023). Figure 3 shows the change in pH of the environment at different current intensities.

The ionic distribution of aluminum and iron when dissolved in water gives us much to understand, as the coagulation process is pH dependent. $Al(OH)_2$ is the first metal hydroxide to be formed at acidic pH. When the OH^- ion concentration increases, $Al(OH)_3$ tends to form equilibria. Moreover, the isoelectric points of the metal hydroxides for Al and Fe electrodes are close to each other at neutral pH or below (Pourabdollah 2021). Cationic iron species such as Fe^{3+}, $Fe(OH)_2$, and $Fe(OH)_3$ may be present in the solution if the hydroxides do not reach a sufficient solubility constant at acidic pH. The iron hydrolysis balance can cause several equilibria compared to the aluminum hydrolysis balance due to the divalent iron. Most importantly, the reduction potential of the Fe^{2+} ions can take place if sufficient oxygen is present in the water.

The increase in the concentration of OH^- ions during electrolysis leads to an increase in the pH value of the wastewater for Al–Al and Fe–Fe electrodes. However, for EO, the increase is less pronounced or in some cases a decrease in pH is observed,

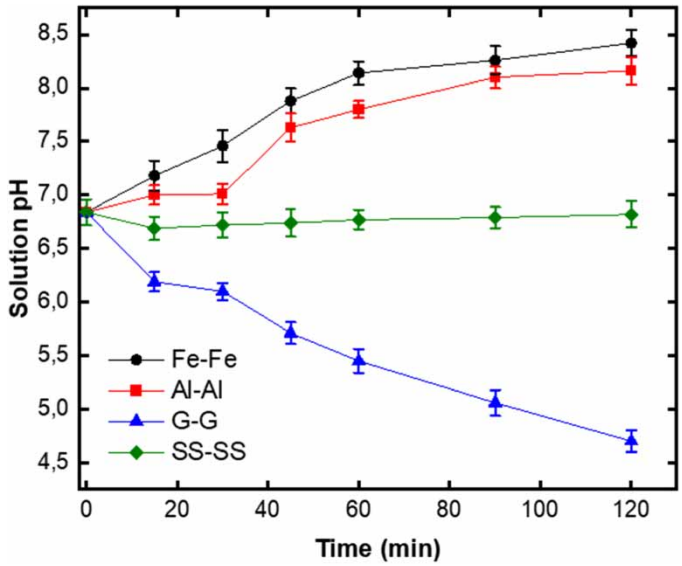

Figure 3 | Variation of pH in the reactor by using Al–Al, Fe–Fe, G–G, and SS–SS.

as in this study. In addition, the release of CO_2 due to hydrogen bubbles that can form on the cathode surface is another reason for the increase in the pH value (Lakshmi & Sivashanmugam 2013). The decrease in pH during electrooxidation can be explained by a possible higher H^+ production compared to OH^-, leading a shift in pH toward the acidic region.

3.1.3. OC evaluation

OCs are an important parameter in wastewater treatment technologies when considering their application on an industrial scale. In this study, the calculation of process cost was therefore estimated only for energy and anode consumption, excluding sludge treatment and maintenance costs. The calculations were based on previous studies (Villasenor-Basulto *et al.* 2022).

The OCs were calculated in the range of \$0.56–30.62/m^3 for the Al electrodes and \$0.07–2.86/m^3 for the G electrodes (Figure 4). These differences in OCs are due to the high voltage value resulting in high power requirements, and this study demonstrates the importance of understanding the requirements. In addition, studies in the literature have shown that uncontrolled pH conditions lead to higher average voltages, which cause high power consumption (Iskurt *et al.* 2020). Overall, the total costs of the processes at different current densities are given in Table 3.

Currently, there is no study in the literature on the electrochemical treatment of wastewater from TP. Therefore, the costs were compared with current literature studies. For example, Isik *et al.* (2020) reported that the cost of treating pistachio wastewater with the EO process via boron-doped diamond (BDD) electrodes is about \$4.38/m^3. In another study by Vidal *et al.* (2019), the EO could be applied for \$1.4/m^3.

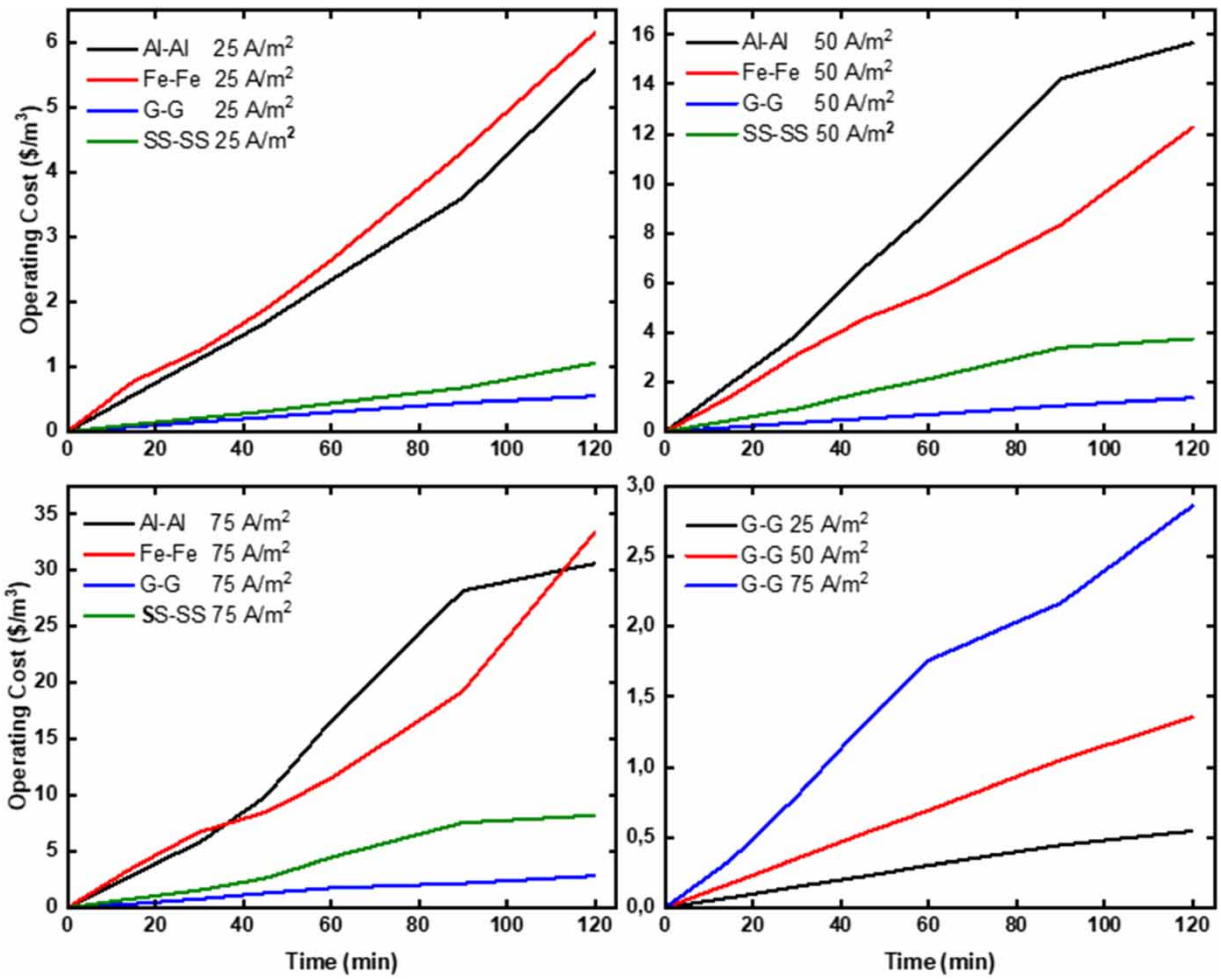

Figure 4 | OC evaluation of electrode pairs corresponds to current density.

Table 3 | Treatment cost of TPW and the efficiencies of EC and EO processes at different current densities (initial pH of 6.84 and electrolysis time of 120 min)

j (A/m^2)	R_{COD}(%)	Cost ($/m^3)	Cost ($/kg COD)
Al–Al			
25	40.5	0.56	1.10
50	63.5	15.69	19.60
75	81.0	30.62	30.02
Fe–Fe			
25	41.3	1.88	3.64
50	46.7	5.55	9.44
75	51.1	33.39	51.85
G–G			
25	28.9	0.07	0.20
50	35.9	0.69	1.54
75	55.5	2.86	4.08
SS–SS			
25	35.4	0.11	0.24
50	43.8	1.56	2.83
75	50.5	8.22	12.92

3.2. Membrane experiment

Under the optimum conditions resulting from the electrochemical treatment (using aluminum electrodes, maintaining the original pH, applying a current density of 75 A/m^2, and performing a 2-h experiment), 1 L of water was prepared for the membrane experiments. These experiments were performed with a volume of 250 mL under 5 bar conditions for each membrane. Samples were taken during the passage of the wastewater through the membranes, and flux measurements were recorded every minute. A COD analysis was then performed after the water obtained from pretreatment was passed through NP030, NP010, and NP90 membranes. Figure 5 shows the permeate flux behavior of wastewater after passing through the NP030, NP010, and NP90 membranes at 5 bars.

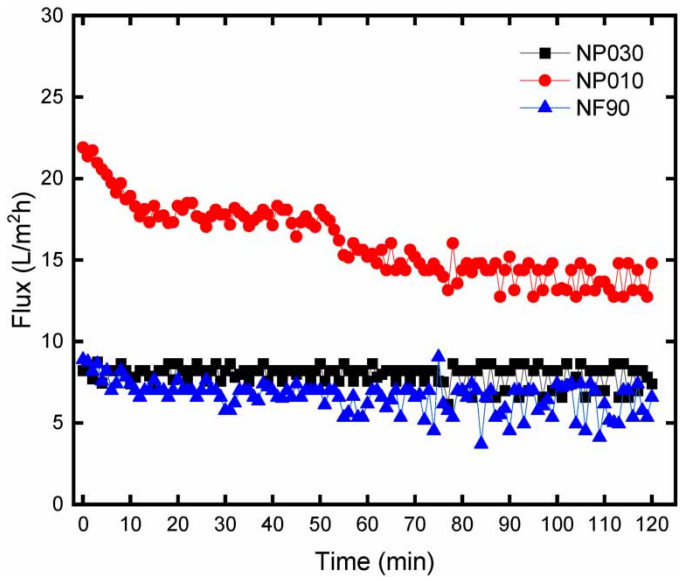

Figure 5 | Flux chart of membrane treatment after pretreated water (experimental conditions: ΔP: 5 bar, pH: 7.0, volume: 250 mL, time: 2 h).

Table 4 | Comparison of combined electrochemical and membrane filtration processes for various pollutant types

		Operating conditions							
Wastewater Type	**Process**	**pH**	**Current density (mA/cm²)**	**Retention time (min)**	**Electrode material**	**Other**	**Removal efficiency**	**OC (US$/m³)**	**Reference**
Wastewater from industrial Cu production	EC + MF	–	48	20	–	–	Se: 98.7%, Cu: 98%, Pb: 98%, As: 99.9%, Zn: 99.9% and Cd: 99.9%	–	Mavrov *et al.* (2006)
Fabric dyeing wastewater	EO + NF	10.6	200	60	Graphite	Flow: 200 m^3/d	SS: 100% and color: 99.4%	2.20	Yildirim *et al.* (2023)
Turnip juice wastewater	EC	5.4	100	45	Al	–	COD: 100% and TPh: 100%	1.58	Arslan *et al.* (2023)
Turnip juice wastewater	EO	5.4	100	45	BDD-Pt	–	COD: 100% and TPh: 100%	0.61	Arslan *et al.* (2023)
Steel wastewater	EC + Fenton	4.0	1.5	25	–	Fe^{2+}/H_2O_2 = 1.5	COD: 98% and TPh: 100%	–	Malakootian & Heidari (2018)
Personal care product wastewater	EC + NF/UF/RO	4.0	500	180	SS	–	COD: 89.6%, surfactant: 99.4% and oil-grease: 99.3%	–	Akarsu *et al.* (2022)
Wet scrubber wastewater	EO + RO	8.0	150	180	Graphite	–	COD: 95% and TPh: 98%		Belibagli *et al.* (2022)
Textile industry wastewater	EC + NF	7.0	2 V	24	Fe	10 ppm celestine blue dye solution	Dye: 79.4%	–	Saad *et al.* (2020)
Poultry processing wastewater	EC + UF	6.7	3	–	Al	Electrodes spacing: 0.9 cm; flow speed: 1.2 L/min, applied pressure: 70 kPa	BOD: 98%, COD: 92% and TSS: 100%	–	Sardari *et al.* (2018)
Hypersaline oil field produced water	EC + MBR	7.2	2.78	120	Al	Electrodes spacing: 5.8 cm	COD: 97% and O&G: 95%	–	Al-Malack & Al-Nowaiser (2018)
Biologically treated textile effluent	EC + NF + RO	8.5	11	90	Fe	Q: 2 L/min, ΔP: 2 bar	COD: 93% and TDS: 91%	–	Güneş & Gönder (2021)
Hospital wastewater	EC + UF	7–8	88.5	60	Al	ΔP: 1 bar	TSS: 95.12% TDS: 97.53% BOD: 95.18% COD: 97.88%	0.89–3.92	Djajasasmita *et al.* (2022)
Hospital wastewater	EC + RO	7–8	110.6 A	60	Al	ΔP: 4 bar	TSS: 97.64% TDS: 99.85% BOD: 97.88% COD: 98.38%	0.93–4.02	Djajasasmita *et al.* (2022)
TP wastewater	EC + NF	6.84	75	120	Al	ΔP: 5 bar	COD: 94% and color: 100%	0.56–30.62	This study

As: arsenic, Cd: cadmium, Cu: copper, MBR: membrane bioreactor, MF: microfiltration, NF: nano-filtration, O&G: oil and grease, Pb: lead, Pt: platinum, RO: reverse osmosis, Se: Selenium, TDS: total dissolved solids, TPh: total phenol, TSS: total suspended solids, UF: ultra-filtration, Zn: zinc.

The initial and steady-state fluxes of pretreated wastewater for the NP030 membrane were 8 and 6.7 L/m^2·h, respectively. For the NP010 and NF90 membranes, the initial fluxes are 20 and 8 L/m^2·h, while the stable fluxes are 15 and 5 L/m^2·h, respectively. Remarkably, no significant decrease in flux was observed for the membranes, which can be attributed to the lower contaminant load of the pretreated water. While the COD value of pretreated wastewater was 240 mg/L, after passing through NP030, NP010, and NP90 membranes, the COD values were 95, 110, and 70 mg/L, respectively. Comparative experimental results of studies on the removal of organic substances and color, as found in the literature, are summarized in Table 4. Additionally, the results of the current study are included.

4. CONCLUSION

In this work, the electrochemical degradation of COD and color from TP wastewater was investigated on a laboratory scale using commonly available and cost-effective electrode materials such as aluminum, iron, graphite, and stainless steel. The aim was to improve the performance of water recovery by treating the pretreated water with the membrane process. Operating parameters such as current density (25–75 A/m^2) and electrolysis time (15–120 min) were also systematically tested. The EC process showed remarkable efficiency, achieving 81% COD and 100% color removal under optimum conditions of 75 A/m^2, pH 6.84, and 120 min using Al–Al electrodes. In contrast, the EO process provided 55.6% COD and 100% color removal efficiency under the conditions of 75 A/m^2 current density, pH 6.84, and 120 min reaction time with G–G electrode pairs. These results emphasize the feasibility of EC and electrooxidation processes for the degradation of organics from TP wastewater, depending on the selection of suitable electrode pairs and operating parameters. The OCs for Al–Al were calculated in the range of 0.56–30.62$, while for BDD-Pt they were in the range of 0.07–2.87 US$/$m^3$. The study conducted with BDD showed a very low dissolution of the electrode as expected, which explains the significant difference in the cost calculation results. In addition, it is worth noting that increasing the current density has a significant impact on the total energy consumption results and therefore influences the first stages of the cost calculation.

Furthermore, the results presented here provide a basis for future research on a combined process as well as for pilot- and real-scale studies. Possible future studies could test mathematical and statistical techniques to further improve and optimize the processes. Three different membranes (NP030, NP010, and NF90) were used to ensure water recovery in the dead-end filtration system operating at a pressure of 5 bar. The initial treatment of the TP wastewater proved to be effective in preventing membrane fouling and a significant drop in flux. The COD removal rates for the NP030, NP010, and NF90 membranes were determined as 92, 91, and 94%, respectively. The results show that water recovery from TP wastewater is achieved with the EC and membrane hybrid system.

FUNDING

This research was supported by the Mersin University Scientific Research Project (BAP), Project no: 2021-2-TP2-4462.

AUTHORS' CONTRIBUTIONS

C.A., H.A., and N.D. contributed to the study conception and design. Material preparation and analysis were performed by A.Ş., Z.B., and C.A. C.A. wrote the manuscript with support from N.D., and all authors commented on previous versions of the manuscript. All authors read and approved the final manuscript.

DATA AVAILABILITY STATEMENT

All relevant data are included in the paper or its Supplementary Information.

CONFLICT OF INTEREST

The authors declare there is no conflict.

REFERENCES

Adou, K. E., Kouakou, A. R., Ehouman, A. D., Tyagi, R. D., Drogui, P. & Adouby, K. 2022 Coupling anaerobic digestion process and electrocoagulation using iron and aluminium electrodes for slaughterhouse wastewater treatment. *Scientific African* **16**, e01238.

Akarsu, C., Deveci, E. Ü., Gönen, Ç. & Madenli, Ö. 2021 Treatment of slaughterhouse wastewater by electrocoagulation and electroflotation as a combined process: Process optimization through response surface methodology. *Environmental Science and Pollution Research International* **28**, 34473–34488.

Akarsu, C., Isik, Z., M'barek, I., Bouchareb, R. & Dizge, N. 2022 Treatment of personal care product wastewater for reuse by integrated electrocoagulation and membrane filtration processes. *Journal of Water Process Engineering* **48**, 102879.

Akbay, H. E. G., Akarsu, C. & Kumbur, H. 2019 Investigation of electrocoagulation process for the removal of phosphate: Full-scale process optimization, operation cost and adsorption kinetics. *Desalination and Water Treatment* **155**, 168–174.

Alam, P. N., Yulianis, Pasya, H. L., Aditya, R., Aslam, I. N. & Pontas, K. 2022 Acid mine wastewater treatment using electrocoagulation method. *Materials Today: Proceedings* **63**, 434–437.

Alghooneh, A., Razavi, S. M. A. & Mousavi, S. M. 2016 Nanofiltration treatment of tomato paste processing wastewater: Process modeling and optimization using response surface methodology. *Desalination and Water Treatment* **57** (21), 9609–9621.

Al-Malack, M. H. & Al-Nowaiser, W. K. 2018 Treatment of synthetic hypersaline produced water employing electrocoagulation-membrane bioreactor (EC-MBR) process and halophilic bacteria. *Journal of Environmental Chemical Engineering* **6**, 2442–2453.

Arslan, H., Gun, M., Akarsu, C., Bilici, Z. & Dizge, N. 2023 Treatment of turnip juice wastewater by electrocoagulation/electroflotation and electrooxidation with aluminum, iron, boron-doped diamond, and graphite electrodes. *International Journal of Environmental Science and Technology* **20**, 53–62.

Asaithambi, P., Aziz, A. R. A. & Bin Wan Daud, W. M. A. 2016 Integrated ozone-electrocoagulation process for the removal of pollutant from industrial effluent: Optimization through response surface methodology. *Chemical Engineering and Processing: Process Intensification* **105**, 92–102.

Belibagli, P., Isik, Z., Özdemir, S., Gonca, S., Dizge, N., Awasthi, M. K. & Balakrishnan, D. 2022 An integrated process for wet scrubber wastewater treatment using electrooxidation and pressure-driven membrane filtration. *Chemosphere* **308**, 136216.

Can, O. T., Kobya, M., Demirbas, E. & Bayramoglu, M. 2006 Treatment of the textile wastewater by combined electrocoagulation. *Chemosphere* **62** (2), 181–187.

Can, B. Z., Boncukcuoglu, R., Yilmaz, A. E. & Fil, B. A. 2014 Effect of some operational parameters on the arsenic removal by electrocoagulation using iron electrodes. *Journal of Environmental Health Science & Engineering* **12**, 95.

Dadari, S., Rahimi, M. & Zinadini, S. 2022 Novel antibacterial and antifouling PES nanofiltration membrane incorporated with green synthesized nickel-bentonite nanoparticles for heavy metal ions removal. *Chemical Engineering Journal* **431**, 134116.

Deghles, A. & Kurt, U. 2016 Treatment of tannery wastewater by a hybrid electrocoagulation/electrodialysis process. *Chemical Engineering and Processing – Process Intensification* **104**, 43–50.

Delil, A. D. & Gönen, N. 2019 Investigation of electrocoagulation and electrooxidation methods of real textile wastewater treatment. *Eskisehir Technical University Journal of Science and Technology A – Applied Sciences and Engineering* **20** (1), 80–91.

Deniz, F. & Akarsu, C. 2018 Operating cost and treatment of boron from aqueous solutions by electrocoagulation in Low concentration. *Global Challenges* **2**, 1800011.

Deveci, E. U., Akarsu, C., Gönen, Ç. & Özay, Y. 2019 Enhancing treatability of tannery wastewater by integrated process of electrocoagulation and fungal via using RSM in an economic perspective. *Process Biochemistry* **84**, 124–133.

Dizge, N., Akarsu, C., Özay, Y., Gulsen, H. E., Adıgüzel, S. K. & Mazmancı, M. A. 2018 Sono-assisted electrocoagulation and cross-flow membrane processes for brewery wastewater treatment. *Journal of Water Process Engineering* **21**, 52–60. https://doi.org/10.1016/j.jwpe.2017.11.016.

Djajasasmita, D., Lubis, S. A. B., Darmawan, I., Pratiwi, D. S. T., Rusgiyarto, F., Nugroho, F. A. & Aryanti, P. T. P. 2022 High-efficiency contaminant removal from hospital wastewater by integrated electrocoagulation-membrane process. *Process Safety and Environmental Protection* **164**, 177–188.

Ebba, M., Asaithambi, P. & Alemayehu, E. 2021 Investigation on operating parameters and cost using an electrocoagulation process for wastewater treatment. *Applied Water Science* **11**, 175.

Esfahani, M. R., Aktij, S. A., Dabaghian, Z., Firouzjaei, M. D., Rahimpour, A., Eke, J., Escobar, I. C., Abolhassani, M., Greenlee, L. F., Esfahani, A. R., Sadmani, A. & Koutahzadeh, N. 2019 Nanocomposite membranes for water separation and purification: Fabrication, modification, and applications. *Separation and Purification Technology* **213**, 465–499.

Figueiredo, D., Ferreira, A., Quelhas, P., Schulze, P. S. C. & Gouveia, L. 2022 *Nannochloropsis oceanica* harvested using electrocoagulation with alternative electrodes – An innovative approach on potential biomass applications. *Bioresource Technology* **344**, 126222.

Gohil, A. & Nakhla, G. 2006 Treatment of tomato processing wastewater by an upflow anaerobic sludge blanket–anoxic–aerobic system. *Bioresource Technology* **97** (16), 2142–2152.

Güneş, E. & Gönder, Z. B. 2021 Evaluation of the hybrid system combining electrocoagulation, nanofiltration and reverse osmosis for biologically treated textile effluent: Treatment efficiency and membrane fouling. *Journal of Environmental Management* **294**, 113042.

Hakizimana, J. N., Gourich, B., Chafi, M., Stiriba, Y., Vial, C., Drogui, P. & Naja, J. 2017 Electrocoagulation process in water treatment: A review of electrocoagulation modelling approaches. *Desalination* **404**, 1–21.

Inan, H., Dimoglo, A., Simsek, H. & Karpuzcu, M. 2004 Olive oil mill wastewater treatment by means of electro-coagulation. *Separation and Purification Technology* **36** (1), 23–31.

Isik, Z., Arikan, E. B., Ozay, Y., Bouras, H. D. & Dizge, N. 2020 Electrocoagulation and electrooxidation pre-treatment effect on fungal treatment of pistachio processing wastewater. *Chemosphere* **244**, 125383. https://doi.org/10.1016/j.chemosphere.2019.125383.

Iskurt, C., Keyikoglu, R., Kobya, M. & Khataee, A. 2020 Treatment of coking wastewater by aeration assisted electrochemical oxidation process at controlled and uncontrolled initial pH conditions. *Separation and Purification Technology* **248**, 117043.

Kabdasli, I., Vardar, B., Arslan-Alaton, I. & Tünay, O. 2009 Effect of dye auxiliaries on color and COD removal from simulated reactive dyebath effluent by electrocoagulation. *Chemical Engineering Journal* **148** (1), 89–96.

Khan, S. U., Khalid, M., Hashim, K., Jamadi, M. H., Mousazadeh, M., Basheer, F. & Farooqi, I. H. 2023 Efficacy of electrocoagulation treatment for the abatement of heavy metals: An overview of critical processing factors, kinetic models and cost analysis. *Sustainability* **15** (2), 1708.

Lakshmi, P. M. & Sivashanmugam, P. 2013 Treatment of oil tanning effluent by electrocoagulation: Influence of ultrasound and hybrid electrode on COD removal. *Separation and Purification Technology* **116** (15), 378–384.

Lynn, W., Heffron, J. & Mayer, B. K. 2019 Electrocoagulation as a pretreatment for electroxidation of *E. coli*. *Water* **11** (12), 2509.

Mahoney, L., Younis, B. A. & Simmons, C. W. 2018 A novel system for the treatment of wastewater from a tomato processing plant with UV light. *Water Practice and Technology* **13** (3), 662–672.

Majidi, S., Erfan-Niya, H., Azamat, J., Cruz-Chú, E. R. & Honore Walther, J. 2022 The performance of a C2N membrane for heavy metal ions removal from water under external electric field. *Separation and Purification Technology* **289**, 120770.

Majlesi, M., Mohseny, S. M., Sardar, M., Gomohammadi, S. & Sheikmohammadi, A. 2016 Improvement of aqueous nitrate removal by using continuous electrocoagulation/electroflotation unit with vertical monopolar electrodes. *Sustainable Environment Research* **26** (6), 287–290.

Malakootian, M. & Heidari, M. R. 2018 Removal of phenol from steel wastewater by combined electrocoagulation with photo-Fenton. *Water Science and Technology* **78** (5–6), 1260–1267. https://doi.org/10.2166/wst.2018.376.

Mannapperuma, J. D., Yates, E. D. & Singh, R. P. 1993 Survey of water use in the California food processing industry. In *Food Industry Environmental Conference*.

Mavrov, V., Stamenov, S., Todorova, E., Chmiel, H. & Erwea, T. 2006 New hybrid electrocoagulation membrane process for removing selenium from industrial wastewater. *Desalination* **201**, 290–296.

Pourabdollah, K. 2021 Simultaneous ε-Keggin Al 13 chloride salt and anionic polyacrylamide coagulation-flocculation system for agglomeration of trimetallic Cr-Ni-Fe doped core-shell microspheres of graphitized coke. *Chemical Engineering Journal* **411**, 128583.

Qasem, N. A. A., Mohammed, R. H. & Lawal, D. U. 2021 Removal of heavy metal ions from wastewater: A comprehensive and critical review. *Clean Water* **4**, 36.

Reilly, M., Cooley, A. P., Tito, D., Tassou, S. A. & Theodorou, M. K. 2019 Electrocoagulation treatment of dairy processing and slaughterhouse wastewaters. *Energy Procedia* **161**, 345–351.

Saad, M. S., Balasubramaniam, L., Wirzal, M. D. H., Abd Halim, N. S., Bilad, M. R., Md Nordin, N. A. H., Adi Putra, Z. & Ramli, F. N. 2020 Integrated membrane – Electrocoagulation system for removal of celestine blue dyes in wastewater. *Membranes* **10** (8), 184.

Safwat, S. M. 2020 Treatment of real printing wastewater using electrocoagulation process with titanium and zinc electrodes. *Journal of Water Process Engineering* **34**, 101137.

Sardari, K., Askegaard, J., Chia, Y., Darvishmanesh, S., Kamaz, M. & Wickramasinghe, S. R. 2018 Electrocoagulation followed by ultrafiltration for treating poultry processing wastewater. *Journal of Environmental Chemical Engineering* **6** (4), 4937–4944.

Tummons, E., Han, Q., Tanudjaja, H. J., Hejase, C. A., Chew, J. W. & Tarabara, V. V. 2020 Membrane fouling by emulsified oil: A review. *Separation and Purification Technology* **248**, 116919.

Vicente, C., Silva, J. R., Santos, A. D., Silva, J. F., Mano, J. T. & Castro, L. M. 2023 Electrocoagulation treatment of furniture industry wastewater. *Chemosphere* **328**, 138500.

Vidal, J., Carvajal, A., Huiliñir, C. & Salazar, R. 2019 Slaughterhouse wastewater treatment by a combined anaerobic digestion/solar photoelectro-Fenton process performed in semicontinuous operation. *Chemical Engineering Journal* **378**, 122097.

Villasenor-Basulto, D., Kadier, A., Singh, R., Navarro-Mendoza, R., Bandala, E. & Peralta-Hernandez, J. M. 2022 Post-tanning wastewater treatment using electrocoagulation: Optimization, kinetics, and settlement analysis. *Process Safety and Environmental Protection* **165**, 872–886.

Wysocka, I. & Masalski, W. 2018 A comparison between the electrocoagulation and the metal dissolution method in the process of phosphorus compounds removal from brewery wastewater. *Environmental Progress & Sustainable Energy* **37**, 975–979.

Yildirim, R., Eskikaya, O., Keskinler, B., Karagunduz, A., Dizge, N. & Balakrishnan, D. 2023 Fabric dyeing wastewater treatment and salt recovery using a pilot scale system consisted of graphite electrodes based on electrooxidation and nanofiltration. *Environmental Research* **234**, 116283.

First received 13 February 2024; accepted in revised form 29 February 2024. Available online 13 March 2024